



### Science Arts & Métiers (SAM)

is an open access repository that collects the work of Arts et Métiers Institute of Technology researchers and makes it freely available over the web where possible.

This is an author-deposited version published in: <https://sam.ensam.eu>  
Handle ID: <http://hdl.handle.net/10985/21517>



This document is available under CC BY license

#### To cite this version :

Robin DURLOT, Francisco J. RESCALVO, Remy FRAYSSINHES, Louis DENAUD, Guillaume POT, Stéphane GIRARDON - An insight into mechanical properties of heartwood and sapwood of large French Douglas-fir LVL - Construction and Building Materials - Vol. 299, p.123859 - 2021

Any correspondence concerning this service should be sent to the repository

Administrator : [scienceouverte@ensam.eu](mailto:scienceouverte@ensam.eu)





# An insight into mechanical properties of heartwood and sapwood of large French Douglas-fir LVL

Robin Duriot<sup>a,\*</sup>, Francisco J. Rescalvo<sup>b</sup>, Guillaume Pot<sup>a</sup>, Louis Denaud<sup>a</sup>, Stéphane Girardon<sup>a</sup>, Remy Frayssinhes<sup>a</sup>

<sup>a</sup> Arts et Metiers Institute of Technology, LaBoMaP, UBFC, HESAM Université, Cluny F-71250, France

<sup>b</sup> Building Engineering School, Department of Applied Physics, University of Granada, Campus Fuentenueva s/n 18071, Granada, Spain

---

## H I G H L I G H T S

---

- Douglas-fir heartwood and sapwood have differentiated mechanical behaviours.
  - Douglas-fir sapwood has relatively comparable performance with industrial LVL product, particularly due to its higher density.
  - Douglas-fir heartwood has lower properties than sapwood, the causes of which are multifactorial like knotiness or juvenile wood variation.
  - Douglas-fir heartwood remains compatible with structural applications.
- 

## A B S T R A C T

The French resource of large diameter Douglas fir is currently still growing, while these large diameter trees are complicated to process efficiently by the sawmilling industry. The rotary peeling process appeared to be particularly adapted as an alternative to the usual sawing. This primary processing method produces veneers used to make a wood engineered product material called Laminated Veneer Lumber (LVL). The manufacturing process of LVL enables the distribution of the resource defects, allowing for increased mechanical behaviour compared to the solid wood from which it comes from. The main objective of this study is to provide an insight into the principal Douglas-fir heartwood LVL mechanical properties such as longitudinal and shear moduli of elasticity, bending, shear and compressive strengths. Up to now, there was no study on LVL derived from this resource. This study focuses on heartwood because of its very interesting natural durability properties for constructive outdoor applications. Moreover, a comparison with structural timber properties and a comparable industrial engineering product, made of Norway spruce and called Kerto<sup>®</sup> S was also achieved to place the material in terms of mechanical performance among the market. Globally, this Douglas-fir heartwood LVL showed high compressive and shear properties. Even though the bending properties were significantly lower than data from Douglas-fir LVL of the literature, they seemed appropriate for structural applications. A larger experimental campaign fully representative of the industrial process and dealing with larger samples will be needed to finally conclude on the characteristic values to be used in structural design.

### Keywords:

Laminated Veneer Lumber  
Douglas-fir  
Heartwood  
Sapwood  
Norway spruce  
Mechanical properties  
Bending  
Compression  
Shear

## 1. Introduction

Douglas-fir (*Pseudotsuga menziesii* (Mirb.) Franco) is a softwood species that originated from the Pacific coast of North America. After two reforestation impulses in the middle of the 19th century

and the second half of the 20th century, France currently has the largest Douglas forest surface in Europe, with about 420,000 ha. In 2018, the harvest volume was around 3 million m<sup>3</sup>. Moreover, Douglas-fir forest resource is increasing significantly [1], since it is estimated that this volume could exceed 6 million m<sup>3</sup> by 2030 [2]. This forecasted increase in volume is essentially due to the increase diameter of the trees. There were already significant quantities of Douglas-fir trees with a diameter of more than 47.5 cm in 2012 [3], and they continue to grow since.

Douglas fir heartwood and sapwood have both a mechanical support role in the tree, but they are very different in moisture

---

\* Corresponding author.

E-mail addresses: [Robin.duriot@ensam.eu](mailto:Robin.duriot@ensam.eu) (R. Duriot), [rescalvo@ugr.es](mailto:rescalvo@ugr.es) (F.J. Rescalvo), [Guillaume.pot@ensam.eu](mailto:Guillaume.pot@ensam.eu) (G. Pot), [Louis.denaud@ensam.eu](mailto:Louis.denaud@ensam.eu) (L. Denaud), [Stephane.girardon@ensam.eu](mailto:Stephane.girardon@ensam.eu) (S. Girardon), [Remy.frayssinhes@ensam.eu](mailto:Remy.frayssinhes@ensam.eu) (R. Frayssinhes).

content [4 5], and important chemical transformations impact the cell wall matrix additive content heartwood conferring its high resistance to insect and fungal attacks, and thus, high durability [6]. Because of these specificities, the potential to exploit Douglas-fir heartwood in outdoor construction without recourse to any treatment is high. Douglas-fir generally has a high proportion of heartwood [7]. This fact combined with the large diameters of the resource lead to an interesting potential of volume of heartwood available to product engineered wood products (EWP) for construction purposes.

However, the absence of pruning for some of these trees leads to the presence of various wood defects such as knots, grain deviation, juvenile wood, and reaction wood which could degrade the mechanical performance of the material [3], and thus restrict the use of large Douglas-fir for structural applications. In addition, large diameters logs cannot be transformed in regular industrial sawmills [8] with canter lines, thus band saw are used, but they present lower yields. Finding an alternative to sawmills and sawn products for this abundant resource, which is reaching its maturity, would participate significantly to optimize its potential.

Laminated veneer lumber (LVL) represents a solution that can deal with these drawbacks. LVL is an EWP, usually used for structural applications such as joist in construction. It is made of a stack of veneers glued together with their grain oriented mainly in the same longitudinal direction [9 10]. These veneers are the result of a primary wood processing operation called rotary peeling, which can easily deal with large diameter logs. The LVL allows for the homogenization of wood defects, such as the knots or resin pockets, in the mass, by a distribution of them inside the entire timber volume. This homogenization of the product avoids the localization of mechanical weakness, and thus allows for homogenized and increased mechanical performance if compared to glulam or solid wood for instance [10 11 12 13 14]. Besides, rotary peeling is also an interesting process to separate heartwood from sapwood efficiently and thus obtaining an EWP made of pure heartwood.

This study is based on French Douglas fir (*Pseudotsuga menziesii* (Mirb.) Franco). This species is still not used in the manufacture of LVL in Europe, where spruce and pine are preferred. Conversely in the USA, Douglas-fir has historically been one of the two the favourite species in the manufacture of LVL material [15]. It is historically very abundant in the country, used primarily for its structural qualities and not for its visual characteristics. Very logically, the literature available is mainly North American. The value of this research study is firstly to be able to compare the mechanical properties of French Douglas-fir LVL with existing Douglas-fir LVL data [10 16 17 18]. The main mechanical loadings studied are bending parallel to the grain; shear and compression parallel and perpendicular to the grain. The second objective is to compare the results between sapwood and heartwood, which can present differentiated mechanical behaviors, but for which no study dealing with LVL was found. This paper present the first large-scale test campaign for the mechanical characterization of an LVL composed from a French Douglas-fir resource.

## 2. Materials and methods

### 2.1. Douglas-fir provenance and peeling

Three different parcels from Corrèze, a French department in the western part of Massif Central, make up the Douglas-fir resource used to compose the LVL panels. The specifications in the choice of the diameter used to compose the panels specified logs with a minimum diameter under bark of 50 cm thin end. A large majority of logs considered were class C and D (low and very low quality according to the standard NF EN 1927-3). At least 7 butt logs and 7 second logs composed each of 3 forest stand resources which are described in Table 1. The veneers are coming from many different trees since only two logs were selected from a tree to get a representative sampling of the resource.

The large total volume of peeled logs (more than 100 m<sup>3</sup>), the variation in silviculture and age of cut were chosen to get as much resource representativeness as possible according to forestry partners experts (AFB and CFBL). All logs were soaked by water aspersion for 48 h to get a temperature of 50 ±2°C before peeling, intending to ease the rotary peeling by increasing the material deformability [19]. Afterward, logs were cut into veneers using a rotary peeling lathe equipped with an automatic centering device, a cylindrical rotating pressure bar adapted to softwood, and a pin drive device. The rotary peeling speed is automatically controlled by the machine. The veneers obtained presented visually a high knottiness. The thickness of each veneer was set to 3.1 mm to reach 3 mm after drying as for Kerto<sup>®</sup> S. The dimensions of each veneer at green state were 2,600 mm × 1300 mm. A resistive moisture content (MC) measurement of each veneer was performed by contact with electrodes directly on the rotary peeling line. This MC assessment allows the selection among the veneers to separate heartwood from sapwood [4]. A veneer with less than 30% MC was automatically identified as heartwood while a veneer with more than 100% MC was identified as sapwood. A second control was involved for veneers with a moisture content value between 30 and 100% MC. In Douglas-fir, the colour is highly differentiated between heartwood (salmon pink) and sapwood (white cream, yellow) [20]; correspondingly, veneers were assimilated to the type of wood which they were closer to in term of colour. Then, the veneers were dried using an industrial air drier to reduce the veneer moisture content to 6% MC. Quality control considering the veneer surface appearance according to EN 635-3 [20] was performed on all veneers using automatic veneer grader from Raute. Veneers of the so-called Q1 superior quality included the classes I, II and III indicated in EN 635-3 [20] standard. Veneers of the so-called lower quality Q2 were Class IV veneers, which may had ingrown knots greater than 60 mm or dead knots greater than 40 mm, splits greater than half the length of the veneer or greater than 15 mm wide or more than 3 splits per metre. Among the 2311 sorted veneers, 1003 made up the sapwood veneer population, which was composed of 36% of Q1 quality veneers and 64% of Q2 quality veneers. 1308 veneers made up the heartwood pop-

**Table 1**  
Forest stands.

	Forest stand 1	Forest stand 2	Forest stand 3
Locality	Larfeuil (Corrèze, France)	Ambrugeat (Corrèze, France)	Neuvic d'Ussel (Corrèze, France)
Average altitude	700 m	700-800 m	600-700 m
Cutting age	65 years	60 years	44 years
Silviculture	Dynamic, planting at 1600 stems/ha, 2 thinnings.	Thinning in 1999, 2 others until the cut.	Dynamic, 1100 stems/ha thinned out at 13 years old in 1983, pruned up to 6 m in 1993, 2 thinnings in 2000 and 2007.
Average ring width	4.0 mm	4.1 mm	6.1 mm

ulation, with 23% of Q1 quality veneers and 77% of Q2 quality veneers.

## 2.2. Panels manufacturing

The Douglas-fir veneers were glued together with the grain orientated parallel to panel length. For a panel, a provenance, a position in the tree (butt logs or second logs), a radial position (sapwood or hardwood) and a veneer quality criterion (Q1 or Q2) are associated when it was possible. In absence of a sufficient number of logs, panels of second logs from forest stand 3, of heartwood second logs from forest stand 2 and of Q1 heartwood second logs from forest stand 3 were not manufactured. The glue used is a phenolic glue spread at 190 g/m<sup>2</sup>; then, the glued veneers were pressed together between 1 and 1.1 MPa for about 30 min in a stage press at 200°C to compose the panel. The final dimensions of the Douglas-fir LVL panels were 2,500 mm × 1250 mm × 45 mm. There were 10 panels purely made from sapwood veneers and 9 heartwood panels. After gluing and pressing, the LVL were stacked and stabilized before being sawn into beams. Concerning Kerto® S LVL [21], 3 panels were ordered from the provider (Metsä Wood Corp.) and used for the manufacturing of specimens. A preliminary study required the sawing of these panels in 2,500 mm × 120 mm × 45 mm beams, thereby conditioning the size of the test specimens in the present study. It is important to note that the Douglas-fir LVL panels were manufactured without any research to homogenize the repartition of defects in the material. As a result, it may have favoured the overlapping of knots through the stacking of veneers.

## 2.3. Samples preparation

In order to measure the bending properties, 133 Douglas-fir and 43 Kerto® S beams (data presented in Table 2) were prepared from the panels with nominal dimensions of 850 mm × 45 mm × 45 mm. Once tested by non-destructive method (explained in the next subsection) and destructive bending testing, both ends of each beam were preserved and sawn to be reused as new specimens for compression and shear tests purpose. Fig. 1 explains the samples extraction from the bending specimen, after failure in 4 points bending, for the subsequent compression and shearing tests. Particular attention has been paid to visually check that no cracks, consequent to the central failure of the beams, have propagated to the reused ends, so it did not affect the mechanical integrity of the material to be tested once again. This is partly why the number of compression and shear samples is lower than the bending ones: it happens that failure spreads to the ends. Moreover, a study on enhancement of LVL bending properties with carbon and basalt fibers reinforcement [22] was carried out in parallel, requiring a number of test specimens. For shear tests, only results from specimen showing 100 per cent cohesive failure in the LVL material were retained.

The specimens taken from the right end of the bending specimens were designed for the longitudinal compression assessment,

**Table 2**  
Samples count summary table.

	French Douglas fir heartwood LVL	French Douglas fir sapwood LVL	Norway spruce LVL Kerto® S
EW bending samples	63	70	43
Parallel to the grain compression samples	34	33	21
Perpendicular to the grain compression samples	40	29	14
Parallel to the grain EW shear samples	17	19	16

measuring 200 mm × 45 mm × 45 mm. Cross section dimensions are in accordance with the minimum section prescribed in EN 14374 standard [9]. The left specimens, measuring 225 mm × 45 mm × 40 mm were used to make parallel to the grain edgewise (EW) shear specimens adapted from EN 789 standard [23]. The 40 mm dimension is due to a 0.1 mm precision planing performed on 2 sides of the specimen to maximize the effectiveness of the loading plates gluing (detailed in section 2.5.2). Four perpendicular to the grain compression samples were taken from each panel. They were 120 mm × 45 mm × 45 mm, cross section dimensions are in accordance with the minimum section prescribed in EN 14374 standard [9]. Concerning compression specimens, the sawing of the specimen faces in contact with the platens has been carried out from the same reference plane in order to guarantee the parallelism of the faces.

Table 2 summarizes the number of specimens for each test.

For each of the tests, all specimens were stored in ambient air. A MC measurement was performed on random samples by resistive pin-type wood moisture meter before non-destructive test, allowing the wood MC to be estimated to be between 7 and 9%.

## 2.4. Non-destructive dynamic measurement

[24] showed that the Timoshenko's bending theory can be applied to determine the dynamic longitudinal modulus of elasticity (*MoE*) and the shear modulus (*G*) from the flexural vibration frequencies in free-free boundary condition. Indeed, they gave the following solution of the equation of motion of a vibrating beam at the first order:

$$\frac{MoE_{dyn-XW}}{\rho} - \frac{MoE_{dyn-XW}}{KG_{dyn-XW}} x_n = y_n \quad (1)$$

where

- $MoE_{dyn-XW}$  is the longitudinal dynamic *MoE* when bending is performed edgewise or flatwise, "XW" being replaced by "FW" or "EW", respectively (Pa)
- $\rho$  is the density (kg/m<sup>3</sup>)
- $K$  is the shear factor ( $K = 5/6$  for a rectangular cross-section)
- $G_{dyn-XW}$  is the dynamic shear modulus when bending is in edgewise or flatwise direction, "XW" being replaced by "FW" or "EW", respectively (Pa)
- $x_n$  and  $y_n$  are parameters depending on the vibrational mode frequency (see [24] for details).

By plotting  $y_n$  against  $x_n$  for different vibration modes, a linear regression allows to identify both the dynamic *MoE* and the shear modulus. The deviation of this equation is generally less than 1% if the length-to-depth ratio is between 10 and 20 from [24] (about 18 in the present work). Based on this theory, the BING device (Beam Identification by Non-Destructive Grading [25]) was used to test all the samples in flatwise (FW) and EW flexural vibrations, and to compute the  $MoE_{dyn-EW}$ ,  $G_{dyn-EW}$ ,  $MoE_{dyn-FW}$ , and  $G_{dyn-FW}$  as shown in Fig. 2. In this paper are presented the following parameters:

$\overline{MoE_{dyn-EW}}$ ,  $\overline{G_{dyn-EW}}$ ,  $\overline{MoE_{dyn-FW}}$  and  $\overline{G_{dyn-FW}}$  mean values of respectively all the  $MoE_{dyn-EW}$ ,  $G_{dyn-EW}$ ,  $MoE_{dyn-FW}$ , and  $G_{dyn-FW}$  values of the population. Indicated in the Eq. (1), solution of the equation of a vibrating beam, the density was required to compute the parameter to identify, and it has to be measured for each beam. Concerning the volume calculation for each beam, height and width dimensions are the means of a 3 different location measuring points performed with a calliper, at both extremes and at the centre of the beam. The accuracy of these two dimensions was +/- 1 mm. The width value was very broadly sensitive to the variability of the thickness of the veneers. The length was measured

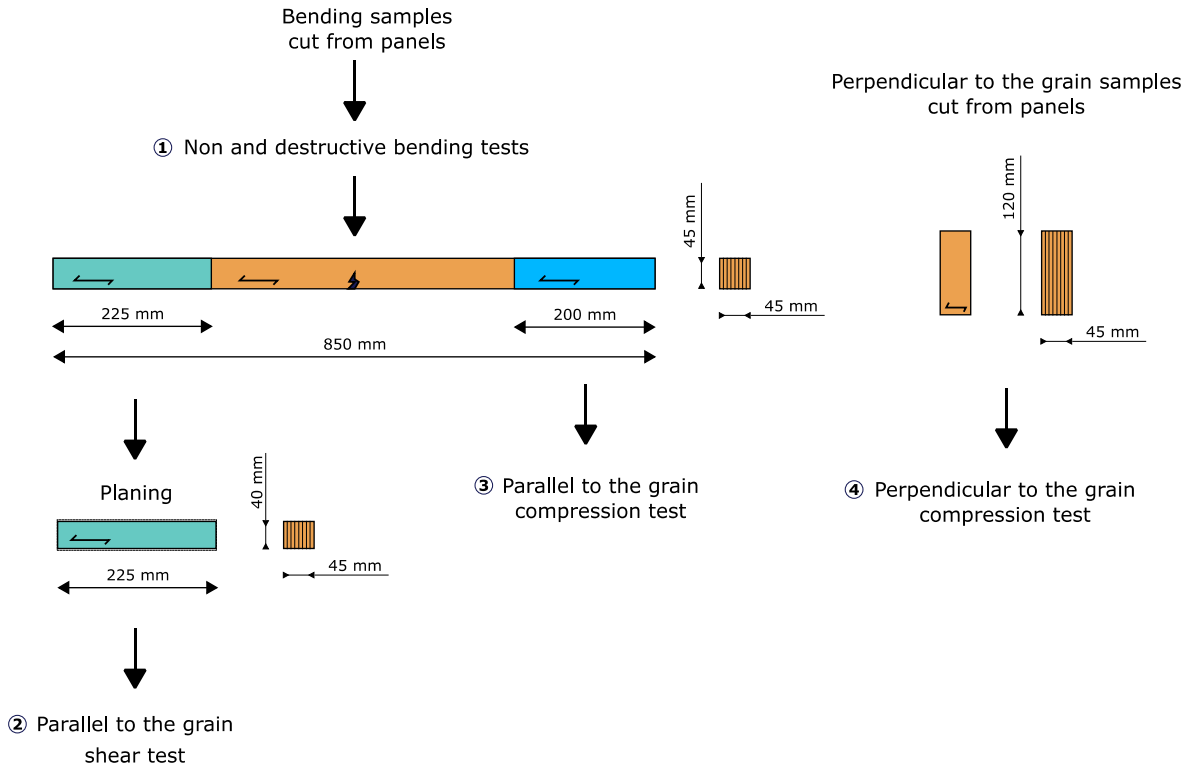


Fig. 1. Cutting samples scheme.

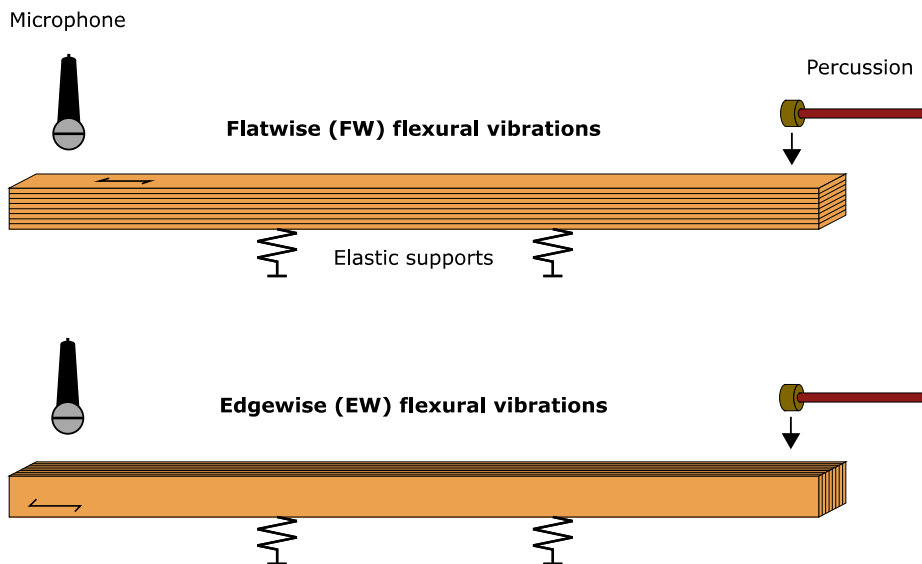


Fig. 2. Beam Bing method testing configurations.

with a measuring tape, with a precision of  $\pm 1$  mm. Mass were measured with a numerical balance with a precision of 0.1 g. Since the density  $\rho$  of each beam was measured,  $\bar{\rho}$ , mean value of all the  $\rho$  of the population was computed for Douglas-fir heartwood (DfH), Douglas-fir sapwood (DfS) and Kerto<sup>®</sup> S (KS).

## 2.5. Destructive tests

### 2.5.1. Bending test set up

After non-destructive testing, a four-points bending test has been performed on every specimen based on the EN 14374 standard [9]. A distance equal to 810 mm, as 18 times the specimen height between the lower supports, was set, as shown in Fig. 3.

The distance between the loading head and the nearest support ( $a$ ) was set to 285 mm, which is 6.33 times the height, in order to prevent possible shear failures. All the specimens were tested in EW direction only. This choice was made to guaranty a sufficient number of successful bending tests in this direction which is the one used for LVL as slender flexural product. Besides, this test configuration presents two advantages for a fair comparison of the material properties: all the plies are subjected substantially to the same mechanical loading, and the glue joints between plies are much less subjected to stresses than in FW bending.

The four-points bending tests were made with a dedicated testing machine composed of an electric actuator, equipped with a 100 kN load sensor, and a global deflection rotary potentiometer

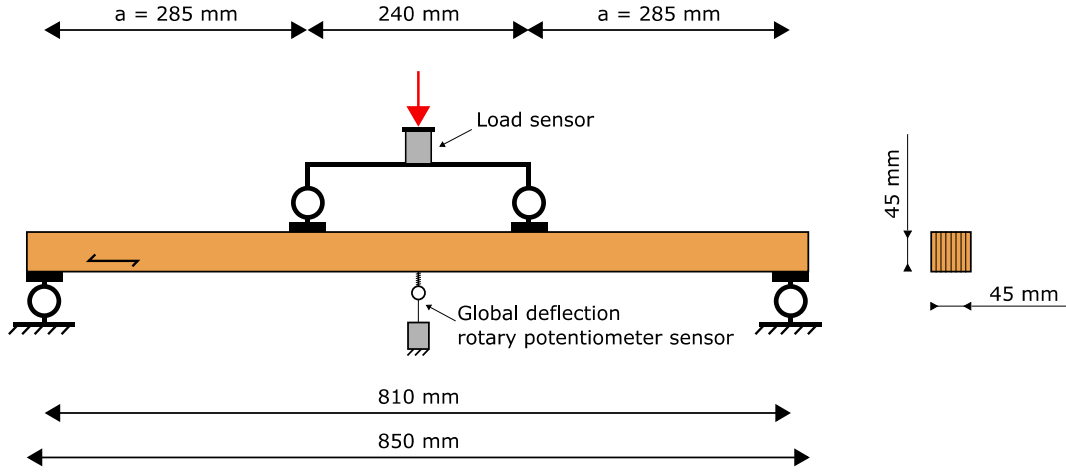


Fig. 3. 4-points bending test arrangement.

sensor. The upper and lower supports were made by 4 cm wide metal plates, fixed on pivot allowing the rotation of the beam supports.

The maximum bending stress ( $\sigma_m$ ) was calculated according to the Eq. (2).

$$\sigma_m = \frac{aF_{m,max}h}{4I_{Gz}} \quad (2)$$

where

- $F_{m,max}$  is the maximum bending effort given by the load sensor (Newton)
- $a$  is the distance between a loading point and the nearest support (mm)
- $h$  is the beam height (mm)
- $I_{Gz}$  is the moment of inertia for a rectangular cross section beam ( $mm^4$ ) defined as  $I_{Gz} = \frac{bh^3}{12}$

The 5th percentile values were calculated according to the method given in EN 14358 standard [26], as recommended in EN 14374 standard [9]. The hypothesis of logarithmic normal or normal distribution has been validated also regarding in EN 14358 standard [26]. Finally, the following parameters were computed:  $\overline{\sigma_m}$ , mean value of all the  $\sigma_m$  values of the population, and  $\sigma_{m,5th}$ , the 5th percentile value for DfH, DfS and KS. Since the density of each beam was measured, the  $S\sigma_m$  specific value was calculated, quotient between  $\sigma_m$  and density  $\rho$ , in order to discuss the influence of density on material performance. Finally,  $\overline{S\sigma_m}$ , mean value of all the  $S\sigma_m$  of the population, were computed for DfH, DfS and KS.

In this study, the global  $MoE$  was used to quantify the stiffness. Although the EN 384 [27] standard provides a formula for adjusting the global modulus of elasticity  $MoE$  to the modulus of elasticity parallel to the grain  $E_0$ , this applies to solid wood, and not for LVL. Then, the global  $MoE$  itself was calculated according to EN 408 + A1 standard [28] by the Equation (3).

$$MoE_{g-EW} = \frac{(3al^2 - 4a^3)(F_2 - F_1)}{48I_{Gz}(V_2 - V_1)} \quad (3)$$

where

- $a$  is the distance between a loading position and the nearest support in a bending test (mm),
- $b$  is the beam width (mm),

- $l$  is the beam length supports (mm)
- $(F_2 - F_1)$  is the increment of load on the linear regression with a correlation coefficient of 0.99 or better (Newton),
- $(w_2 - w_1)$  is the increment of deformation corresponding to  $F_2 - F_1$ , measured by the local deflection LVDT sensor (mm),
- $(V_2 - V_1)$  is the increment of displacement measured by the rotary potentiometer corresponding to  $F_2 - F_1$  (mm).

Finally,  $\overline{MOE_{g-EW}}$ , mean value of all the  $MOE_{g-EW}$  values of the population and  $\overline{SMOE_{g-EW}}$ , mean value of all the  $MoE_{g-EW}$  specific values ( $SMOE_{g-EW}$ ) were both computed for DfH, DfS and KS.

#### 2.5.2. Parallel to the grain EW shear test set up

Shear tests were made with a universal testing machine, which loads the samples by uniaxial compression. The whole shearing test set-up is described in Fig. 4. It was composed of a frame and a crosshead, which provide a maximal load capacity of 250 kN. For parallel to the grain EW shear tests, the set up used was taken

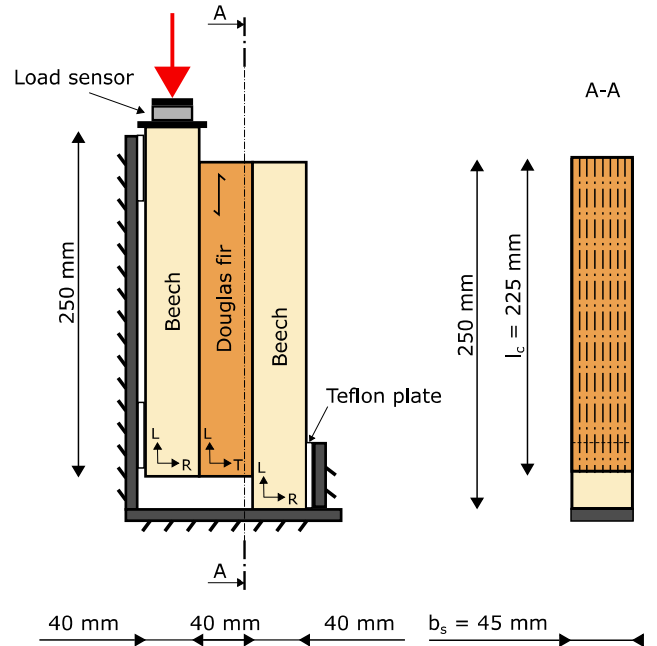


Fig. 4. Scheme of shear test arrangement.

from the EN 789 standard [23]. Originally designed for planar shear properties testing, the work-holding device and test specimen principle were here used for shear testing in EW plane. The major disadvantage of the asymmetric specimen shape is the eccentricity of the applied load generated. This leads to a slight parasitic bending moment in the proof body. A work-holding device was therefore necessary to minimize this phenomenon. It was made up of 2 orthogonal metallic plane elements, providing plane support for the two elements made up by beech. The specimen was stopped in translation in a plane perpendicular to the loading direction by an adjustable stop held in place by clamp screws, tightened upon contact with the test body. PTFE plates were in use to reduce the friction between the work-holding device and the specimen during the loading. The whole shearing test set-up is described in Fig. 4. Two 250 mm × 45 mm × 45 mm beech elements have been prepared to replace the steel plates advised in the standard (but not mandatory). This species was chosen for its excellent stiffness in the RL plan and superior to the intended strength range for the species tested. The glue used to bond the beech elements to the specimen is a white vinyl glue. The surfaces of beech elements were planed down and double-gluing technique was operated to maximize the quality and strength of the bonding. In accordance with the manufacturer's requirements, a pressure of 1 MPa was applied by a mechanical press during a minimum of 6 h, and a curing time of at least 48 h was performed for each specimen.

Maximum parallel to the grain EW shear stress was calculated according to the Eq. (4).

$$\sigma_{v,0} = \frac{F_{v,0,max}}{l_s b_s} \quad (4)$$

where

- $F_{v,0,max}$  is the maximum parallel to the grain shear effort given by the load sensor (Newton)
- $b_s$  is the width of the LVL test specimen (mm)
- $l_s$  is the length of the LVL test specimen (mm)

Finally, the following parameters were computed:  $\overline{\sigma_{v,0}}$ , mean value of all the  $\sigma_{v,0}$  values of the population, and  $\sigma_{v,0,5th}$ , the 5th percentile value for DfH, DfS and KS.

### 2.5.3. Parallel compression test and perpendicular to the grain EW compression test set up

Compression tests were made with the same universal testing machine than the previous part. To perform parallel and perpendicular to the grain compression test, 2 parallel-plane bearing plates were used. The maximum parallel to the grain compressive stress was calculated according to the Eq. (5).

$$\sigma_{c,0} = \frac{F_{c,0,max}}{A} \quad (5)$$

where

- $F_{c,0,max}$  is the maximum parallel to the grain compressive effort given by the load sensor (Newton)
- $A$  is the cross-sectional area (mm<sup>2</sup>)

And the maximum perpendicular to the grain compressive stress was calculated according to the Eq. (6).

$$\sigma_{c,90} = \frac{F_{c,90,max}}{A} \quad (6)$$

where

- $F_{c,90,max}$  is the maximum perpendicular to the grain compressive effort given by the load sensor (Newton), determined using 1% deformation offsetting slope process from EN 408 + A1 standard [28]

Finally, the following parameters were computed:  $\overline{\sigma_{c,0}}$ , mean value of all the  $\sigma_{c,0}$  values of the population, and  $\sigma_{c,0,5th}$ , the 5th percentile value,  $\overline{\sigma_{c,90}}$ , mean value of all the  $\sigma_{c,90}$  values of the population, and  $\sigma_{c,90,5th}$ , the 5th percentile value, for DfH, DfS and KS.

## 3. Results and discussions

All along the paper, the results are presented in tables according to the formality presented in Table 3.

A Tukey HSD test has been performed to compare average mechanical properties relative to each other. Populations submitted to an HSD test (Tukey method) are signalled in the following tables by a letter. Lowercase letters are used when the test was performed on specific values; capital letters are used on raw values.

### 3.1. Elastic bending properties

Table 4 shows the results of the vibratory and destructive tests (test n°1 in Fig. 1) in terms of dynamic MoE in EW and FW bending and global MoE in EW bending for each beam. Specific modulus SMOE was calculated for each case.

$MOE_{g-EW}$  measured in destructive EW bending tests showed good similarities in observed trends with  $MOE_{dyn-EW}$ , both in relative gaps between means and coefficients of variation. However, it is noted that  $MOE_{g-EW}$  mean values were systematically lower than  $MOE_{dyn-EW}$ . This could be explained because no correction in the global MoE formula including shear deformations between upper and lower supports has been applied as it is done for sawn timber according to EN 384 standard. The observed systematic difference was not particularly surprising, since the measurement of MoE is actually a complex subject for a heterogenous material as wood. The interested reader can refer to [29] for more details on the subject. Other factors are also involved, such as compression in support areas in destructive test.

In terms of  $\bar{\rho}$ , a difference of about 51 kg/m<sup>3</sup> was notable between DfH (544 kg/m<sup>3</sup>) and DfS (595 kg/m<sup>3</sup>). This is a finding that has already been made in previous works [30]. A variation in pith-to-bark density confirming this trend was also observed on Douglas-fir from New-Zealand in the work of [31 32]. A differentiated mature wood/juvenile wood effect could be a very likely cause. The density of KS was measured at 525 kg/m<sup>3</sup>. This mean value was indeed lower than the measured mean densities of Douglas-fir, which was expected for a product made from Norway spruce. Yet, it was 15 kg/m<sup>3</sup> higher than the  $\bar{\rho}$  of 510 kg/m<sup>3</sup> provided by the manufacturer [33] for 12% MC. As the MC range measured in this study was strictly lower than this reference, lower

**Table 3**  
Property table architecture.

Experimental results		
French Douglas fir heartwood LVL (DfH)	French Douglas fir sapwood LVL (DfS)	Norway spruce LVL Kerto® S (KS)
Value (CoV %) XX	Value (CoV %) XX	Value (CoV %) XX
Relative difference of DfH compared to DfS %	Relative difference of DfS compared to KS %	
Relative difference of DfH compared to KS %		

**Table 4**  
Density, dynamic and global MoE properties.

Test	Loading direction	Property	Statistical indicators	Experimental results		
				French Douglas fir heartwood LVL	French Douglas fir sapwood LVL	Norway spruce LVL Kerto® S
Non-destructive test	Flexural FW	Density $\rho$ (kg/m <sup>3</sup> )	Mean (CoV %)	544 (4) B – 8.6% + 3.7%	595 (5) A + 13.4%	525 (3) C
		MoE <sub>dyn-FW</sub> (GPa)	Mean (CoV %)	13.7 (11.8) D – 15.9% – 11.3%	16.3 (9.2) AB + 5.4%	15.4 (7.7) C
		S <sub>MoE</sub> <sub>dyn-FW</sub> (Mm <sup>2</sup> .s <sup>-2</sup> )	Mean (CoV %)	25.1 (9.8) d – 8.1% – 14.5%	27.3 (7.4) c – 7.0%	29.4 (5.9) ab
	Flexural EW	MoE <sub>dyn-EW</sub> (GPa)	Mean (CoV %)	13.2 (10.3) D – 20.4% – 11.9%	16.5 (8.2) A + 10.7%	14.9 (7.8) C
		S <sub>MoE</sub> <sub>dyn-EW</sub> (Mm <sup>2</sup> .s <sup>-2</sup> )	Mean (CoV %)	24.2 (9.0) d – 13.0% – 15.0%	27.8 (6.7) c – 2.3%	28.5 (6.0) abc
		MoE <sub>g-EW</sub> (GPa)	Mean (CoV %)	12.3 (11.1) E – 20.8% – 14.0%	15.5 (8.0) B + 8.6%	14.2 (6.8) C
Destructive test	Flexural EW	S <sub>MoE</sub> <sub>g-EW</sub> (Mm <sup>2</sup> .s <sup>-2</sup> )	Mean (CoV %)	22.6 (9.7) e – 13.3% – 16.8%	26.0 (5.8) c – 4.1%	27.1 (5.1) b

Values followed by a different letter within a column are statistically different at p-value = 5% (ANOVA and Tukey HSD test).

densities would have been expected. Consequently, this difference can be attributed to Norway Spruce provenance itself.

$\overline{MoE}_{dyn-EW}$  value of 14.9 MPa found for the KS is consistent with the 13.8 MPa provided by the manufacturer, according to the respective MCs and considering the higher mean density.

According to the Tukey's HSD test, there was no significant difference between  $\overline{MoE}_{dyn-FW}$  and  $\overline{MoE}_{dyn-EW}$  for DfH, DfS and KS at 5% level: the stiffnesses were the same in both bending directions on average, as expected for a random repartition of the defects. The CoV were, however, higher for  $\overline{MoE}_{dyn-FW}$ , may be due to the preponderant influence of edge veneers on stiffness on FW. Indeed, in EW bending, each layer can be considered as independent, allowing the global stiffness of the material to be determined as the sum of the stiffness of each veneer. In contrast, in FW bending, the positioning of each veneer has a much greater influence on the overall mechanical properties because each layer is subjected to different stress rates, depending on whether it is placed near the neutral fibre or on the edges. This phenomenon has already been studied in [34]. Therefore, the quality of exterior veneers has a strong impact on MoE. For DfH and DfS LVL, the lack of optimization of veneer location therefore implied a greater variability of stiffness in FW than in EW direction (11.8% vs 10.3% for DfH, 9.2% vs 8.2% for DfS). For KS, Metsä Wood Corp. has sorting specifications for face veneers for its Kerto® products, limiting knot size and minimizing the number of defects per unit volume [35]. The results of this study show that CoV in FW and EW were almost identical (7.7% vs. 7.8%). The influence of the quality of face veneers is therefore a very compelling explanation.

In EW and FW bending configurations, the KS  $MoE_{dyn}$  mean values were systematically included between a DfS and DfH mean values, respectively the superior and inferior limits. To make hypotheses about the cause of this trend, the calculation of the specific moduli  $\overline{S_{MoE}_{dyn}}$  allows to observe material stiffness by removing the effect of the density. As a result, the hierarchy of the materials according to their stiffness changes. The KS was systematically placed at the top of the range in terms of specific modulus (in FW, the relative difference between DfS and KS decreases from + 5.4% to – 7.0%). DfH retained lower performances than DfS, but the difference was reduced by its lower density than DfS

(544 kg/m<sup>3</sup> versus 595 kg/m<sup>3</sup>). Particularly in EW position, the relative difference went from – 20.4% to – 13.0% for specific value. Density has obviously a significant effect on the stiffnesses, explaining partly the differences between heartwood (juvenile wood effect) and sapwood of Douglas-fir wood, and also KS.

The remaining gap of performance between DfH and DfS could be explained partly by a difference in terms of size and number of knots per unit of volume. The presence of knots implies a higher local grain angle variation, which decreases the global material stiffness according to the global grain direction of the veneers. In the literature, higher number of knots was observed in DfH close to the pith [36] than towards the periphery of the tree, where DfS is located but where a greater diameter is observed. In this study, 64% of DfS veneers were sorted as Q2 quality vs 77% for DfH. This can explain why are more important for DfH than DfS: the hypothesis behind this phenomenon is a direct dependence of modulus on wood defects.

The obtained  $MoE_{dyn}$  values were relatively high, corresponding, on the basis of structural timber grades of EN 338, to the stiffness of classes C35 ( $E_{m,0,mean}$  of 13.0 GPa), C50 (16.0 GPa) and C40 (14.0 GPa) for DfH, DfS and KS, respectively [37]. This being higher or at least equal to the highest sawn timber grades currently used in structural applications. According to Table 5 from [38], the mean stiffness values determined in the destructive test of this study are consistent with what already exists in the literature. DfS was within the range of stiffnesses measured for Douglas-fir LVL, while DfH was lower, but remained in a range of already measured values. As a result, the obtained MoE for LVL made of large French

**Table 5**  
Literature Douglas-fir LVL global MoE mean values.

	Raw material quality	EW (GPa)	FW (GPa)
Jung (1982)	Low to High	15.5–19.2	15.4–19.3
	Random	17.6	16.6
Kunesh (1978)	C and D	15.9	16.1
Kretschmann and others (1993)	/	9.0–12.8	9.0–13.7
Hesterman and others (1992)	/	15.3	



Douglas-fir seem promising, and may excel the values needed for structural design.

### 3.2. Bending strength

The calculated maximum stresses, result of destructive bending tests (test n°1 in Fig. 1), are presented in this part and summed up in Table 6.

Concerning  $\bar{\sigma}_m$ , DfS and KS were not significantly different (respectively 74.2 MPa and 73.5 MPa), while DfH was almost one-third less resistant (49.7 MPa). A smaller knottiness can explain this result because it can reduce the probability of a weakening knot in a volume of beam that can prematurely initiate the failure phenomenon. As a result, this tend to favour DfS over DfH. A collateral effect to greater knottiness in a material is a larger CoV in strength results. Indeed, this increases the probability of interlayer overlapping of knots, favouring low-stress failure, but some specimen can still also present high-stress failure. This effect of knots overlay in Douglas-fir materials due to the lack of optimization of defect distribution in the multi-layers induces low  $\bar{\sigma}_m$  and large CoV, which highly impacts the 5th percentile value. Indeed, the difference in  $\sigma_{m,5th}$  between the DfS and DfH was important (DfS value was 2 times higher than DfH). DfH, exhibited  $\sigma_{m,5th}$  value of 32.9 MPa, compared to 55.2 MPa for DfS, and 60.8 MPa for KS.

A calculation of the specific maximum stress,  $\bar{S}\bar{\sigma}_m$  mean values was performed. Between DfS and KS, the difference between mean values increased from +0.9% in  $\bar{\sigma}_m$  to -11.1% in  $\bar{S}\bar{\sigma}_m$  but between DfS and DfH, the difference went from -33.0% mean value to -28% specific mean value. This allows to notice that density did not explain differentiated behaviour at failure between DfH and DfS LVL.

It should be noticed that, given the low height of the beams tested (45 mm) and the known existence of size effects, this study does not allow for a formal conclusion on the results of strengths to be used in structural design, but it draws trends in terms of maximum stresses and relative differences between materials. Indeed, a difference of -40.4% between DfH and DfS is observed. The calculated 5th percentile value of maximum stress of DfH is comparable to a C24 class, by recalculating its resistance (30.97 MPa) for a height of 45 mm and taking into account the test configuration via the 2 adjustment factors ( $k_h$  of 1.27 and  $k_l$  of 1.01) given by EN 384 [27]. Although being lower than other LVL products, the 5th percentile strength value of DfH LVL would seem sufficient for structural purpose. As a result, the obtained strength seems interesting, especially considering the quality of the wood in use, because if the same wood material has been sawn, it would likely not had fulfilled the strength grading requirements for structural use (because of knots localized in the same region inducing high stress concentrations).

**Table 6**  
Maximum stresses measured by bending test.

Property	Statistical indicators	Experimental results		
		French Douglas fir heartwood LVL	French Douglas fir sapwood LVL	Norway spruce LVL Kerto® S
$\sigma_m$ (MPa)	Mean (CoV %)	49.7 (21.9) B -33.0% -32.5%	74.2 (14.2) A +0.9%	73.5 (10.1) A
	5th percentile	32.9 -40.4% -45.9%	55.2 -9.2%	60.8
$S\sigma_m$ (Mm <sup>2</sup> .s <sup>-2</sup> )	Mean (CoV %)	0.090 (24.073) c -28.0% -36.0%	0.125 (12.678) b -11.1%	0.140 (9.420) a

Values followed by a different letter within a column are statistically different at p-value = 5% (ANOVA and Tukey HSD test).

### 3.3. Shear properties

#### 3.3.1. Shear moduli

Table 7 shows the results of the vibratory test (test n°1 in Fig. 1) in terms of dynamic shear modulus measured in EW and FW bending for each beam.

Regardless of the species,  $\bar{G}_{dyn}$  were systematically higher in EW than in FW position (+15.0% for DfH, +15.8% for DfS, +18.8% for KS). For KS, this hierarchy is consistent with data provided by Metsä Wood Corp. in [21] with a  $G_{0,EW,mean}$  of 600 MPa and a  $G_{0,FW,mean}$  of 380 MPa. It is the result of intrinsic shear stiffness properties of the Norway spruce species, which differ according to the direction of orthotropy considered in the tree. The shear modulus measured in FW bending involves a stiffness property in the radial-longitudinal plan whereas the one arising from EW bending involves a stiffness property in the tangential-longitudinal plan. On the contrary to Norway spruce, the hierarchy between  $G_{RL}$  and  $G_{TL}$  shear moduli for Douglas-fir clear wood differ according to sources [39-38]. In this study for which wood with important defects was in use, a  $\bar{G}_{dyn-EW}$  greater than  $\bar{G}_{dyn-FW}$  was observed.[40] had pointed out that veneer lathe checks should penalize more LVL shear moduli in EW than in FW direction, but this did not appear in this results.

The same trend as for MoE remains for the CoV of  $\bar{G}_{dyn}$  values by species: highest for DfH and lowest for KS, again demonstrating the influence of resource variability. The shear moduli of the Douglas-fir were found to be much superior to KS (15.1% on EW). Again, this relies to the intrinsic stiffness properties of the species. However, DfH and DfS shear moduli were not significantly different, and much superior to KS one (+19% on FW and +14% on EW). By calculating the specific values of the shear moduli, DfH values became significantly higher than DfS and KS. This behaviour may be explained by the greater presence of larger knots that deflect the fiber orientation, which could actually improve the shear stiffness of DfH against DfS.

Therefore, it appears that the variation in values between species and between DfH and DfS was multifactorial, which had already been mentioned by [41]. This potentially depends on lathe checks characteristics (frequency and depth), proportion and size of knots, and the effect of growth rings [42], which limits the interpretation of these results. However, it is clear that these Douglas-fir LVL samples present very good shear stiffness properties, comparable at least to a EN338 C30 class [37] ( $G_{mean}$  of 750 MPa) when loaded in FW as in EW direction.

#### 3.3.2. Parallel to the grain ew shear strength

The measured maximum shear stresses ( $\bar{\sigma}_{v,0}$ ) obtained in the parallel to the grain EW shear tests (test n°2 in Fig. 1) are presented in Table 8. For shear and compression strength results, specimen mass was not measured, which not allow to show specific values.

**Table 7**  
Dynamic shear modulus.

Position	Property	Statistical indicators	Experimental results		
			French Douglas fir heartwood LVL	French Douglas fir sapwood LVL	Norway spruce LVL Kerto® S
Flexural FW direction	$G_{\text{dyn-FW}}$ (MPa)	Mean (CoV %)	789 (18) B −0.5% +17.5%	793 (13) B +18.1%	671 (10) C
	$SG_{\text{dyn-FW}}$ ( $\text{Mm}^2 \cdot \text{s}^{-2}$ )	Mean (CoV %)	1.45 (17.73) b +8.8% +13.3%	1.33 (10.86) c +4.1%	1.28 (8.54) c
Flexural EW direction	$G_{\text{dyn-EW}}$ (MPa)	Mean (CoV %)	907 (17) A −1.2% +13.8%	918 (10) A +15.1%	797 (8) B
	$SG_{\text{dyn-EW}}$ ( $\text{Mm}^2 \cdot \text{s}^{-2}$ )	Mean (CoV %)	1.67 (15.60) a +8.2% +9.5%	1.54 (7.78) b +1.3%	1.52 (8.75) b

Values followed by a different letter within a column are statistically different at p-value = 5% (ANOVA and Tukey DHS test).

All  $\overline{\sigma_{v,0}}$  means for all three tested LVLs were not significantly different between them (at 5% level). The same remark as for shear modulus applies here for the absence of difference between DfH and DfS mean shear strength: this behaviour is difficult to interpret and is certainly multifactorial, the variation in knotiness between the materials in this study notably not being identified. In terms of 5th percentile values, DfH mean value is like other mechanical properties penalized by a higher CoV than the KS one, which results in lower 5th percentile values.

In the literature, [17] present a comparable Douglas-fir mean value of 5.38 MPa (CoV of 20%) with EW parallel to the grain shear test for a Douglas-fir LVL classified as low quality, manufactured in Canada with no distinction between sapwood and heartwood. Likewise, a mean value of 5.90 MPa is found in [18] for North American interior Douglas-fir. Based on the results of these tests, DfH is comparable to a C20 class ( $f_{v,0,k}$  of 3.6 MPa). If it appears to be an issue, this could be managed by the use of cross layers which increase EW shear strength as in some existing industrial products [43]. DfS would correspond to all classes beyond C24 class ( $f_{v,0,k}$  of 4.0 MPa) [37], which is quite remarkable. It can be noticed there is a 5th percentile strength value of 4.25 MPa for KS very close to the 4.2 MPa given by the manufacturer by EN 408 test.

### 3.4. Compression strength

Two tests were performed to characterize the LVL materials: parallel and perpendicular to the grain compression. Only the strengths were measured in these destructive tests (displacements were not measured on the samples).

#### 3.4.1. Parallel to the grain compression strength

Strength results (test n°3 in Fig. 1) are presented by values in Table 9.

**Table 8**  
Parallel to the grain edgewise shear strengths.

Property	Statistical indicators	Experimental results		
		French Douglas fir heartwood LVL	French Douglas fir sapwood LVL	Norway spruce LVL Kerto® S
$\sigma_{v,0}$ (MPa)	Mean (CoV %)	5.33 (16.5) A −3.0% +0.7%	5.50 (13.2) A +3.8%	5.30 (10.0) A
	5th percentile	3.62 −11.6% −14.8%	4.10 −3.7%	4.25

Values followed by a different letter within a column are statistically different at p-value = 5% (ANOVA and Tukey DHS test).

The  $\overline{\sigma_{c,0}}$  value for DfS was higher than DfH one (54.2 MPa versus 46.9 MPa), but not significantly different from KS (52.6 MPa) at 5% level. The CoV were still much more important for Douglas-fir, especially for DfH, which had a  $\sigma_{c,0,5th}$  of 33.3 MPa. The DfH mean value was close from North American interior Douglas fir mean value of 48.27 MPa in [18]. DfS and KS remained very close together (respectively 46.0 MPa and 47.0 MPa). Logically, it is noted that these trends were very similar to what can be observed with the results of bending strength presented before. The higher CoV of DfH compared to DfS could probably also be explained by the fact that DfH contains both juvenile and mature wood. Since density plays a major role in compressive strength, this has the effect of making a high CoV. The general higher knotiness of Douglas-fir compared to spruce may also explain why, despite a higher density, DfS only slightly exceeds KS. However, the compression strength values found for Douglas-fir are very promising since they were over all classes presented in EN 338 [37] (C50 to  $f_{c,0,k}$  of 30 MPa).

#### 3.4.2. EW perpendicular to the grain compression strength

Strength results (test n°4 in Fig. 1) are presented by values in Table 10.

The  $\overline{\sigma_{c,90}}$  values for DfH and KS (respectively 7.13 MPa and 7.70 MPa) were not significantly different at 5% level. DfS  $\overline{\sigma_{c,90}}$  value was much higher than the other ones (9.24 MPa), but had a very large CoV. The DfH mean value was close from North American interior Douglas fir mean value of 7.03 MPa in [18]. As explained before for perpendicular to the grain compression strength, it could be assumed that the mature wood/juvenile wood in DfH induced this larger CoV. Relative gaps between Douglas-fir and KS are less than those calculated for parallel to the grain compression, which may potentially be due to a reinforcing effect of the nodes in the perpendicular to the grain direction. This has the effect of ranking it between DfH and KS in terms of 5th per-

**Table 9**  
Parallel to the grain compression strengths.

Property	Statistical indicators	Experimental results		
		French Douglas fir heartwood LVL	French Douglas fir sapwood LVL	Norway spruce LVL Kerto® S
$\sigma_{c,0}$ (MPa)	Mean (CoV %)	46.9 (15.2) B −13.5% −10.8%	54.2 (8.1) A + 3.0%	52.6 (5.6) A
	5th percentile	33.7 −26.8% −28.3%	46.0 −1.9%	47.0

Values followed by a different letter within a column are statistically different at p-value = 5% (ANOVA and Tukey HSD test).

**Table 10**  
Perpendicular to the grain compression stresses.

Property	Statistical indicator	Experimental results		
		French Douglas fir heartwood LVL	French Douglas fir sapwood LVL	Norway spruce LVL Kerto® S
$\sigma_{c,90}$ (MPa)	Mean (CoV %)	7.13 (15.3) B −22.9% −7.5%	9.24 (19.5) A +20.0%	7.70 (7.7) B
	5th percentile	5.13 −12.9% −21.4%	5.89 −9.8%	6.53

Values followed by a different letter within a column are statistically different at p-value = 5% (ANOVA and Tukey DHS test).

centile values. For KS, the  $\sigma_{c,90,5th}$  of 6.53 MPa is very close to the reference value  $f_{c,90,EW,k}$  of 6 MPa provided by the supplier in [21]. One hypothesis to explain the good results of Douglas-fir LVL could be its greater thickness of latewood in comparison with Norway Spruce [44]. This characteristic thus implies a greater proportion of tracheids of smaller diameter and greater thickness than in earlywood, which is particularly beneficial to the performance in this loading. The performance of DfH and DfS in compression perpendicular to grain was again well above all the classes presented in EN 338 [37] (the C50 characteristic value  $f_{c,0,k}$  is 3.2 MPa), which leads to a very good ranking of the Douglas-fir LVL's EW compression behaviour when compared to the structural requirements.

#### 4. Conclusions

This paper is the first to deal with the valorization of large French Douglas-fir into a LVL material and the comparison of its mechanical characteristics with its high-performance North American counterparts, European Norway spruce LVL, or structural sawn timber. It provides a good insight into French Douglas-fir LVL mechanical properties, but it should be kept in mind in the interpretation of the results that (1) the specimens were of smaller size than the reference width of the European standards, (2) the specimen came from a semi-industrial process, (3) the sampling was chosen to be as representative as possible of the french resource but was still not comparable to an industrial production. However, considering there is no LVL Douglas production in Europe, this sample is really large for a first scientific approach.

The LVL material produced from heartwood of these Douglas fir trees showed high shear and compressive properties, but the bending properties were significantly lower than an industrial LVL product obtained from Norway spruce (Kerto® S) tested in the same conditions: the 5th percentile bending stress was 32.5% lower and the mean MoE was 11.9% lower in EW direction. However, these bending properties are compatible with structural purposes (32.9 MPa of 5th percentile bending strength for a 45 mm thick beam). This result is especially interesting, considering the fact that the strength grading of Douglas-fir sawn timber generally leads to low yields, thus more added value could be obtained with LVL products than sawn products from the same resource [45]. It is

also worth reminding that this product would exhibit natural durability allowing its usage for specific applications for which there would be no other LVL product competitor on the market.

Apart from the shear properties, significant differences in mechanical properties (stiffness and strength) were observed between the Douglas-fir LVL made of sapwood and the one made of heartwood. These differences can be explained by the higher density and lower number of knots of sapwood *i.e.*, wood far from the pith. The LVL product made from sapwood of Douglas-fir had measured mechanical properties that exceeded or competed with industrial Norway spruce LVL. As a result, this material could be of high interest when the natural durability is not a criterion, thus for the same current applications as Norway spruce LVL (structural purpose inside buildings).

Sapwood showed high strengths although generally having CoV slightly higher than Kerto® S. Regarding heartwood, higher dispersions were observed. This was expected in a material where the probability of interlayer knot overlap is increased for a wood material with more knots per unit volume. This dispersion could be reduced by a proper sorting of the veneer, which can be imagined on a peeling line equipped of non-destructive measurement devices.

#### CRediT authorship contribution statement

**Robin Duriot:** Conceptualization, Investigation, Validation, Formal analysis, Writing - original draft, Visualization. **Francisco J. Rescalvo:** Conceptualization, Investigation. **Guillaume Pot:** Conceptualization, Methodology, Supervision, Writing - review & editing, Validation. **Louis Denaud:** Supervision, Writing - review & editing. **Stéphane Girardon:** Supervision, Writing - review & editing. **Remy Frayssinhes:** Investigation.

#### Declaration of Competing Interest

The authors declare that they have no known competing financial interests or personal relationships that could have appeared to influence the work reported in this paper.

## Acknowledgements

This study is funded by the region of Burgundy Franche-Comté, France Douglas, Thebault Group and the Spanish COMPOP Timber project (No. BIA2017-82650-R). This work was completed thanks to the Technical Platform Xylomat, subsidized by ANR-10-EQPX-16 XYLOFOREST. Thanks to Florent Aparé for his investment in the experimental task during his Master project period.

## References

- [1] IGN, 'La forêt plantée en France: état des lieux', 2017. [https://inventaire-forestier.ign.fr/IMG/pdf/if40\\_plantations.pdf](https://inventaire-forestier.ign.fr/IMG/pdf/if40_plantations.pdf) (accessed Oct. 29, 2020).
- [2] 'Le Douglas – 2. Ressource', France Douglas. <https://www.france-douglas.com/le-douglas/ressource.html> (accessed Oct. 29, 2020).
- [3] 'Importance et rôles des gros et très gros bois en France', Pro Silva, 2012. <https://prosilva.fr/img/fichiers/etude-gros-bois-2011-v27.pdf>.
- [4] F. Mothe, R. Marchal, and W. T. Tatischeff, 'Heart dryness of Douglas fir and ability to rotary cutting: research of alternative boiling processes. 1. Moisture content distribution inside green wood and water impregnation with an autoclave', *Annals of Forest Science (France)*, 2000, Accessed: Oct. 29, 2020. [Online]. Available: <https://agris.fao.org/agris-search/search.do?recordID=FR2000003808>.
- [5] R. Frayssinhes, S. Girardon, B. Marcon, L. Denaud, R. Collet, A Simple Method to Determine the Diffusivity of Green Wood, *Bioresources* 15 (Aug. 2020) 6539–6549, <https://doi.org/10.15376/BIORES.15.3.6539-6549>.
- [6] 'Les principales caractéristiques technologiques de 245 essences forestières tropicales – Douglas', *Tropix* 7, 2012. <https://tropix.cirad.fr/FichiersComplementaires/FR/Temperees/DOUGLAS.pdf> (accessed Oct. 29, 2020).
- [7] 'Le Douglas, un choix naturel pour la construction', France Douglas. <https://www.france-douglas.com/assets/components/francedouglas/images/mediatheque/catalogues/construction.pdf> (accessed Oct. 29, 2020).
- [8] R. Collet and L. Bleron, 'Perspectives de valorisation et de transformation du douglas en Bourgogne', *Forêt Entreprise*, vol. 188, pp. 27–31, Sep. 2009.
- [9] 'NF EN 14374 (mars 2005) : Structures en bois – LVL (Lamibois) – Exigences', 2005. <https://www.batipedia.com.rp1.ensam.eu/pdf/document/QTH.pdf#zoom=100> (accessed Mar. 25, 2019).
- [10] LVL Handbook Europe. Federation of the Finnish Woodworking Industries, 2019.
- [11] A. Ranta-Maunus, M. Fonselius, J. Kurkela, T. Toratti, *Reliability analysis of timber structures*, VTT Technical Research Centre of Finland (2001).
- [12] A. Ranta-Maunus, J. K. Denzler, and P. Stapel, 'Strength of European Timber. Part 2. Properties of spruce and pine tested in Gradewood project', p. 115, 2011.
- [13] 'Timber Design Guide 2007 – Timber Design'. <https://www.timberdesign.org.nz/design-aids/timber-design/timber-design-guide-2007/> (accessed Oct. 29, 2020).
- [14] H. Ido, H. Nagao, H. Kato, A. Miyatake, Y. Hiramatsu, Strength properties of laminated veneer lumber in compression perpendicular to its grain, *J Wood Sci* 56 (5) (Oct. 2010) 422–428, <https://doi.org/10.1007/s10086-010-1116-3>.
- [15] R. P. Vlosky, P. M. Smith, P. R. Blankenhorn, and M. P. Haas, 'Laminated Veneer Lumber: A United States Market Overview', *Wood and Fiber Science*, vol. 26, no. 4, Art. no. 4, 1994.
- [16] T. L. Laufenberg, 'Parallel-laminated veneer: processing and performance research review', *Forest Products Journal (USA)*, 1983, Accessed: Oct. 29, 2020. [Online]. Available: <https://agris.fao.org/agris-search/search.do?recordID=US8295306>.
- [17] J. C. Bohlen, 'Shear strength of douglas-fir laminated-veneer lumber', *Forest products journal*, 1975, Accessed: Oct. 29, 2020. [Online]. Available: <https://agris.fao.org/agris-search/search.do?recordID=US201302714341>.
- [18] N. D. Hesterman and T. M. Gorman, 'Mechanical properties of laminated veneer lumber made from interior Douglas-fir and lodgepole pine', *Forest products journal (USA)*, 1992, Accessed: Oct. 29, 2020. [Online]. Available: <https://agris.fao.org/agris-search/search.do?recordID=US9327253>.
- [19] R. Frayssinhes, S. Stefanowski, L. Denaud, S. Girardon, B. Marcon, and R. Collet, 'Peel Veneer from Douglas-Fir: Soaking Temperature Influence on the Surface Roughness', Aug. 2019.
- [20] 'NF EN 635-3 (1995-07-01): Plywood. Classification by surface appearance. Part 3 : softwood.', 1995. <https://sagaweb-afnor-org.rp1.ensam.eu/fr-FR/sw/consultation/notice/1244973?recordfromsearch=True> (accessed Oct. 29, 2020).
- [21] MetsäWood and P. O. Box, 'Declaration of performance – Kerto LVL S-beam – Structural Laminated Veneer Lumber', vol. N° MW/LVL/311-001/CPR/DOP, p. 3, 2019.
- [22] Francisco J. Rescalvo, Robin Duriot, Guillaume Pot, Antolino Gallego, Louis Denaud, Enhancement of bending properties of Douglas-fir and poplar laminate veneer lumber (LVL) beams with carbon and basalt fibers reinforcement, *Constr. Build. Mater.* 263 (2020) 120185, <https://doi.org/10.1016/j.conbuildmat.2020.120185>.
- [23] 'NF EN 789 (2005-04-01): Timber structures – Test methods – Determination of mechanical properties of wood based panels'. <https://sagaweb-afnor-org.rp1.ensam.eu/fr-FR/sw/consultation/notice/1277070?recordfromsearch=True> (accessed Oct. 29, 2020).
- [24] L. Brancheriau, H. Bailleres, Natural vibration analysis of clear wooden beams: a theoretical review, *Wood Sci. Technol.* 36 (4) (Aug. 2002) 347–365, <https://doi.org/10.1007/s00226-002-0143-7>.
- [25] 'Non-destructive testing of wood'. <https://www.picotech.com/library/application-note/non-destructive-testing-of-wood> (accessed Oct. 29, 2020).
- [26] 'NF EN 14358 (2016-12-23): Timber structures – Calculation and verification of characteristic values'. <https://sagaweb-afnor-org.rp1.ensam.eu/fr-FR/sw/consultation/notice/1413569?recordfromsearch=True> (accessed Oct. 29, 2020).
- [27] 'NF EN 384+A1 (2018-11-21): Structural timber – Determination of characteristic values of mechanical properties and density'. <https://sagaweb-afnor-org.rp1.ensam.eu/fr-FR/sw/consultation/notice/1539784?recordfromsearch=True> (accessed Oct. 29, 2020).
- [28] 'NF EN 408+A1 (2012-09-01): Timber structures – Structural timber and glued laminated timber – Determination of some physical and mechanical properties'. <https://sagaweb-afnor-org.rp1.ensam.eu/fr-FR/sw/consultation/notice/1401191?recordfromsearch=True> (accessed Oct. 29, 2020).
- [29] D. Gil-Moreno, D. Ridley-Ellis, and P. McLean, 'Using the rigth modulus of elasticity to get the best grades out of softwood timber species in Great Brintain', 2016, p. 9.
- [30] Fleur Longuetaud, Frédéric Mothe, Philippe Santenoise, Ndiaye Diop, Jana Dlouha, Meriem Fournier, Christine Deleuze, Patterns of within-stem variations in wood specific gravity and water content for five temperate tree species, *Annals of Forest Science* 74 (3) (2017), <https://doi.org/10.1007/s13595-017-0657-7>.
- [31] S. Cardoso, H. Pereira, Characterization of Douglas-fir grown in Portugal: heartwood, sapwood, bark, ring width and taper, *Eur J Forest Res* 136 (4) (Aug. 2017) 597–607, <https://doi.org/10.1007/s10342-017-1058-z>.
- [32] Mark O. Kimberley, Russell B McKinley, David J. Cown, John R. Moore, Modelling the variation in wood density of New Zealand-grown Douglas-fir, *N. Z. J. For. Sci.* 47 (1) (2017), <https://doi.org/10.1186/s40490-017-0096-0>.
- [33] 'Kerto(R) LVL S-beam Datasheet', MetsäWood. <https://www.metsawood.com/global/tools/materialarchive/materialarchive/metsawood-kerto-s-french.pdf> (accessed Oct. 29, 2020).
- [34] S. Girardon, L. Denaud, G. Pot, I. Rahayu, Modelling the effects of wood cambial age on the effective modulus of elasticity of poplar laminated veneer lumber, *Annals of Forest Science* 73 (3) (Sep. 2016) 615–624, <https://doi.org/10.1007/s13595-016-0569-y>.
- [35] 'Kerto(R) manual LVL – Visual properties'. <https://www.metsawood.com/global/Tools/MaterialArchive/MaterialArchive/Kerto-manual-lvl-visual-properties.pdf> (accessed Oct. 29, 2020).
- [36] I. Robert Kliger, Mikael Perstorper, Germund Johansson, *Bending properties of Norway spruce timber. Comparison between fast- and slow-grown stands and influence of radial position of sawn timber*, *Annales des sciences forestières* 55 (3) (1998) 349–358.
- [37] 'NF EN 338 (2016-07-01): Structural timber – Strength classes'. <https://sagaweb-afnor-org.rp1.ensam.eu/fr-FR/sw/consultation/notice/1413267?recordfromsearch=True> (accessed Oct. 29, 2020).
- [38] Forest Products Laboratory and United States Department of Agriculture, Forest Service, Wood Handbook, Wood as an Engineering Material, General Technical Report FPL-GTR-190, Madison, WI, 2010.
- [39] D. Guitard, *Mécanique du matériau bois & composites*, Cépaduès. (1987).
- [40] G. Pot, L. Denaud, and R. Collet, 'Numerical study of the influence of veneer lathe checks on the elastic mechanical properties of laminated veneer lumber (LVL) made of beech', *Holzforschung*, vol. 0, Jan. 2014, doi: 10.1515/hf-2014-0011.
- [41] C.Y.C. Purba, G. Pot, J. Viguier, J. Ruelle, L. Denaud, The influence of veneer thickness and knot proportion on the mechanical properties of laminated veneer lumber (LVL) made from secondary quality hardwood, *Eur. J. Wood Prod.* 77 (3) (May 2019) 393–404, <https://doi.org/10.1007/s00107-019-01400-3>.
- [42] F. Mothe, 'Aptitude au déroulage du bois de Douglas : conséquences de l'hétérogénéité du bois sur la qualité des placages', These de doctorat, Vandoeuvre-les-Nancy, INPL, 1988.
- [43] 'Kerto(R) LVL Q-panel Datasheet', MetsäWood. <https://www.metsawood.com/global/Tools/MaterialArchive/MaterialArchive/MW-KertoLVL-Qpanel-datasheet-FR.pdf> (accessed Oct. 29, 2020).
- [44] G. Nepveu and J.-L. Blachon, 'Ring width and its suitability for use in studies on the structure of several conifers : Douglas fir, Scots pine, maritime pine, Sitka spruce, Norway spruce, silver fir', 1989. <https://doi.org/10.4267/2042/26001>.
- [45] J. Viguier, D. Bourreau, J.-F. Bocquet, G. Pot, L. Bléron, J.-D. Lanvin, Modelling mechanical properties of spruce and Douglas fir timber by means of X-ray and grain angle measurements for strength grading purpose, *Eur. J. Wood Wood Prod.* 75 (4) (Jan. 2017) 527–541, <https://doi.org/10.1007/s00107-016-1149-4>.